

# META-AGGREGATING NETWORKS FOR CLASS-INCREMENTAL LEARNING

Yaoyao Liu<sup>1</sup>, Bernt Schiele<sup>1</sup>, Qianru Sun<sup>2</sup>

<sup>1</sup> Max Planck Institute for Informatics, <sup>2</sup> Singapore Management University  
{yaoyao.liu, schiele}@mpi-inf.mpg.de qianrusun@smu.edu.sg

## ABSTRACT

Class-Incremental Learning (CIL) aims to learn a classification model with the number of classes increasing phase-by-phase. The inherent problem in CIL is the stability-plasticity dilemma between the learning of old and new classes, i.e., high-plasticity models easily forget old classes but high-stability models are weak to learn new classes. We alleviate this issue by proposing a novel network architecture called Meta-Aggregating Networks (MANets) in which we explicitly build two residual blocks at each residual level (taking ResNet as the baseline architecture): a stable block and a plastic block. We aggregate the output feature maps from these two blocks and then feed the results to the next-level blocks. We meta-learn the aggregating weights in order to dynamically optimize and balance between two types of blocks, i.e., between stability and plasticity. We conduct extensive experiments on three CIL benchmarks: CIFAR-100, ImageNet-Subset, and ImageNet, and show that many existing CIL methods can be straightforwardly incorporated on the architecture of MANets to boost their performance<sup>1</sup>.

## 1 INTRODUCTION

AI systems are expected to work in an incremental manner when the amount of knowledge increases over time. They should be capable to learn new concepts while maintaining the ability to recognize previous ones. However, deep-neural-network-based systems often suffer from serious forgetting problems (usually called “catastrophic forgetting”) when continuously updated using new coming data. This is due to two facts: (i) the updates can override the knowledge acquired from the previous data (McCloskey & Cohen, 1989; McRae & Hetherington, 1993; Ratcliff, 1990; Shin et al., 2017; Kemker et al., 2018); and (ii) the model can not replay the entire previous data to regain the old knowledge. To encourage the study to addressing the forgetting problems, Rebuffi et al. (2017) defined a class-incremental learning (CIL) protocol that requires the model to do image classification for which the training data of different classes come in a sequence of phases. In each phase, the classifier is re-trained on new class data, and then evaluated on the test data of both old and new classes. To prevent trivial algorithms such as storing all old data for replaying, there is a strict memory budget — only a tiny set of exemplars of old classes can be saved in the memory.

This memory constraint causes the serious data amount imbalance between old and new classes, and indirectly causes the main problem of CIL – stability-plasticity dilemma (Mermillod et al., 2013). Higher plasticity results in the forgetting of old classes (McCloskey & Cohen, 1989), while higher stability weakens the model from learning the data of new classes (containing a larger number of samples). Existing methods try to balance stability and plasticity using simple data strategies. As illustrated in Figure 1, they directly train the model on the imbalanced dataset (Rebuffi et al., 2017; Li & Hoiem, 2018), and some other works include a fine-tuning step using a balanced subset of exemplars (Castro et al., 2018; Hou et al., 2019; Douillard et al., 2020). However, these methods turn out to be not particularly effective. For example, LUCIR (Hou et al., 2019) sees an accuracy drop of around 16% in predicting 50 previous classes in the last phase (compared to the upper-bound accuracy when all old samples are available) on the CIFAR-100 dataset (Krizhevsky et al., 2009).

In this paper, we address the stability-plasticity dilemma by introducing a novel network architecture called Meta-Aggregating Networks (MANets) for CIL. Taking the ResNet (He et al., 2016b) as

<sup>1</sup>Code: <https://github.com/yaoyao-liu/class-incremental-learning>

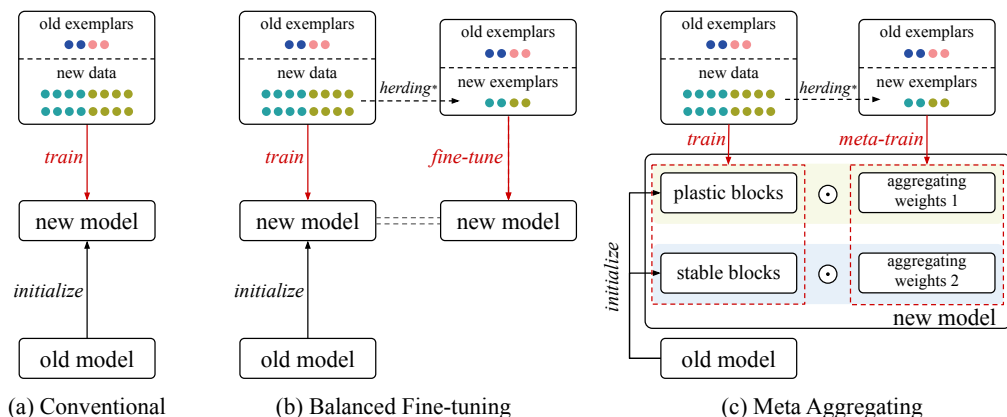


Figure 1: Conceptual illustrations of different CIL methods. (a) Conventional methods use all available data (imbalanced classes) to train the model (Rebuffi et al., 2017; Hou et al., 2019) (b) Castro et al. (2018), Hou et al. (2019) and Douillard et al. (2020) follow the convention but add a fine-tuning step using the balanced set of exemplars. (c) Our MANets approach uses all available data to update the plastic and stable blocks, and use the balanced set of exemplars to meta-learn the aggregating weights. We continuously update these weights such as to dynamically balance between plastic and stable blocks, i.e., between plasticity and stability. \*: *herding* is the method to choose exemplars (Welling, 2009), and can be replaced by other methods, e.g., *Mnemonics Training* (Liu et al., 2020).

an example of baseline architectures, in MANets, we explicitly build two residual blocks (at each residual level): one for maintaining the knowledge of old classes (i.e., the stability) and the other for learning new classes (i.e., the plasticity), as shown in Figure 1(c). We achieve these by allowing different numbers of learnable parameters in these two blocks, i.e., less learnable parameters in the stable but more in the plastic. We apply aggregating weights to the output feature maps from these two blocks, sum them up, and pass the results to the next residual level. In this way, we are able to dynamically balance between the stable and plastic features, i.e., stability and plasticity, by updating the aggregating weights. To achieve auto updating, we take these weights as hyperparameters and use meta-learning (Finn et al., 2017; Wu et al., 2019; Liu et al., 2020) to optimize them.

Technically, the optimization of MANets includes two steps at each CIL phase: (1) learn the network parameters for two types of residual blocks, and (2) meta-learn their aggregating weights. Step 1 is the standard training for which we use all the data available at the phase. Step 2 aims to balance between two types of blocks for which we downsample the new class data to build a balanced subset as the meta-training data, as illustrated in Figure 1(c). We formulate these two steps in a bilevel optimization program (BOP) and conduct the optimizations alternatively, i.e., update network parameters with aggregating weights fixed, and then switch (Sinha et al., 2018; MacKay et al., 2019; Liu et al., 2020). For evaluation, we conduct extensive CIL experiments on three benchmarks, CIFAR100, ImageNet-Subset, and ImageNet. We find that many existing CIL methods, e.g., iCaRL (Rebuffi et al., 2017), LUCIR (Hou et al., 2019), Mnemonics Training (Liu et al., 2020), and PODNet (Douillard et al., 2020), can be straightforwardly incorporated on the architecture of MANets, yielding consistent performance improvements.

**Our contributions** are thus three-fold: (1) a novel and generic network architecture consisting of stable and plastic blocks, specially designed for tackling the problems of CIL; (2) a BOP-based formulation and the corresponding end-to-end optimization solution that enables dynamic and auto balancing between stable and plastic blocks; and (3) extensive experiments by incorporating the proposed architecture into different baseline methods of CIL.

## 2 RELATED WORK

**Incremental learning** studies the problem of learning a model from the data that come gradually in sequential training phases. It is also referred to as continual learning (De Lange et al., 2019a; Lopez-Paz & Ranzato, 2017) or lifelong learning (Chen & Liu, 2018; Aljundi et al., 2017). Re-

cent approaches are either in task-incremental setting (classes from different datasets) (Li & Hoiem, 2018; Shin et al., 2017; Hu et al., 2019; Chaudhry et al., 2019; Riemer et al., 2019), or in class-incremental setting (classes from the identical dataset) (Rebuffi et al., 2017; Hou et al., 2019; Wu et al., 2019; Castro et al., 2018; Liu et al., 2020). **Our work** is conducted on the setting of the latter one we call class-incremental learning (CIL). Incremental learning approaches can be categorized according to the methods of tackling the problem of model forgetting. There are regularization-based, replay-based, or parameter-isolation-based methods (De Lange et al., 2019b; Prabhu et al., 2020). **Regularization-based** methods introduce regularization terms in the loss function to consolidating previous knowledge when learning new data. Li & Hoiem (2018) first applied the regularization term of knowledge distillation (Hinton et al., 2015) in CIL. Hou et al. (2019) introduced a series of components such as less-forgetting constraint and inter-class separation to mitigate the negative effects caused by data imbalance (between old and new classes). Douillard et al. (2020) proposed an efficient spatial-based distillation-loss applied throughout the model and a representation comprising multiple proxy vectors for each class. **Replay-based** methods store a tiny subset of old data, and replay the model on them together with the new class data. Rebuffi et al. (2017) picked the nearest neighbors of the average sample per class for the subset. Liu et al. (2020) parameterized the samples in the subset and meta-optimized them in an end-to-end manner. **Parameter-isolation-based** methods are mainly applied to task-incremental learning (not CIL). Related methods dedicate different model parameters for different incremental phases, to prevent model forgetting (caused by parameter overwritten). Abati et al. (2020) equipped each convolution layer with task-specific gating modules which select specific filters to learn current input. Rajasegaran et al. (2019) progressively chose the optimal paths for the new tasks meanwhile encouraging parameter sharing across tasks. **Our work** is the first one proposing new network architecture for CIL. We isolate the knowledge of old classes and the learning of new classes specially in two types of residual blocks, and meta-learn their weights to balance between them automatically.

**Meta-learning** can be used to optimize hyperparameters of deep models, e.g., the aggregating weights in our MANets. Technically, the optimization process can be formulated as a bilevel optimization program where model parameters are updated at the base level and hyperparameters at the meta level (Von Stackelberg & Von, 1952; Wang et al., 2018; Goodfellow et al., 2014). Recently, there emerge a few of meta-learning based incremental learning methods. Wu et al. (2019) meta-learned a bias correction layer for incremental learning models. Liu et al. (2020) parameterized data exemplars and optimized them by meta gradient descent. Rajasegaran et al. (2020) incrementally learned new tasks while meta-learning a generic model to retain the knowledge of all training tasks.

### 3 META-AGGREGATING NETWORKS (MANets)

Class incremental learning (CIL) usually assumes there are  $(N + 1)$  learning phases in total, i.e. one initial phase and  $N$  incremental phases during which the number of classes gradually increases (Hou et al., 2019; Liu et al., 2020; Douillard et al., 2020). In the initial phase, only data  $\mathcal{D}_0$  is available to train the first model  $\Theta_0$ . There is a strict memory budget in CIL systems, so after the phase, only a small subset of  $\mathcal{D}_0$  (exemplars denoted as  $\mathcal{E}_0$ ) can be stored in the memory to used as replay samples in later phases. In the  $i$ -th ( $i \geq 1$ ) phase, we load the exemplars of old classes  $\mathcal{E}_{0:i-1} = \{\mathcal{E}_0, \dots, \mathcal{E}_{i-1}\}$  to train model  $\Theta_i$  together with new class data  $\mathcal{D}_i$ . Then, we evaluate the trained model on the test data containing both old and new classes. We repeat such training and evaluation through all phases.

The major challenge of CIL is that the model trained at new phases easily “forgets” old classes. To tackle this, we introduce a novel architecture called MANets. MANets is based on ResNet and each of its residual levels is composed of two different blocks: a plastic one to adapt to the new class data and a stable one to maintain the knowledge learned from old classes. The details of this architecture are provided in Section 3.1. The optimization steps of MANets are elaborated in Section 3.2.

#### 3.1 THE ARCHITECTURE OF MANets

In Figure 2(a), we provide an illustrative example of our MANets with three residual levels. The inputs  $x^{[0]}$  are the images and the outputs  $x^{[3]}$  are the features for training classifiers. Every residual level in-between consists of two parallel residual blocks: one (orange) will be actively adapted to new coming classes while the other one (blue) has its parameters partially fixed to maintain the

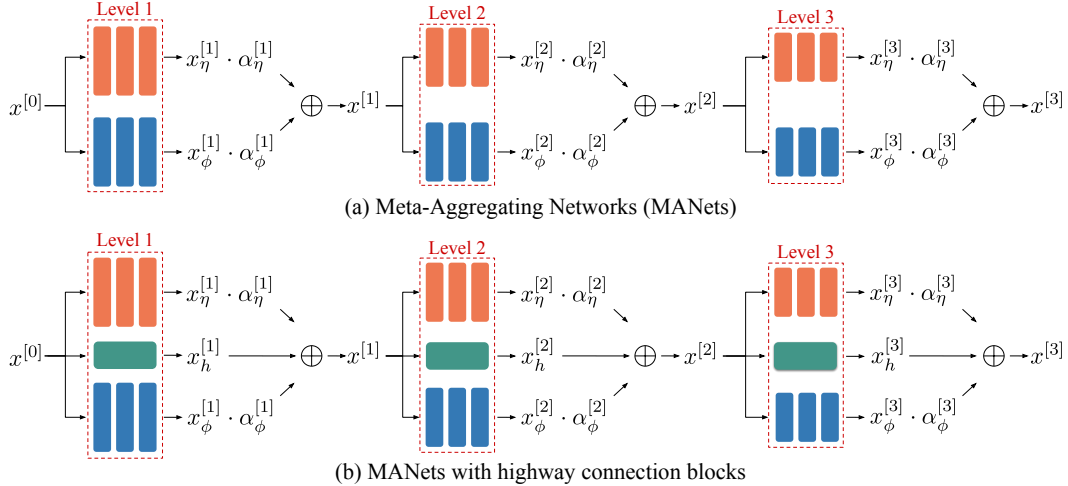


Figure 2: (a) The architecture of MANets. For each residual level, we derive the feature maps from stable blocks ( $\phi \odot \theta_{\text{base}}$ , blue) and plastic blocks ( $\eta$ , orange), respectively, aggregate them with meta-learned weights, and feed the result in the next level. (b) An improved version of MANets by including a highway connection block ( $h$ , green) at each level.

knowledge learned from old classes. After feeding images to Level 1, we obtain two sets of feature maps respectively from two blocks, and aggregate them by weight parameters  $\alpha^{[1]}$ . Then, we feed the resulted maps to Level 2 and repeat the steps above. The same applies to Level 3. Finally, we pool the resulted maps after Level 3 to learn classifiers. In addition, Figure 2(b) provides an improved version of MANets by including a highway connection block (green) at each residual level. Below we discuss (i) the design and benefits of the dual-branch residual blocks; (ii) the operations for feature extraction and aggregation; and (iii) the design and benefits of highway connection blocks.

**Stable and plastic blocks at each residual level.** We aim to balance between the plasticity (for learning new classes) and stability (for maintaining the knowledge of old classes) using a pair of stable and plastic blocks at each residual level. We achieve this by allowing different numbers of learnable parameters in two blocks, i.e., less learnable parameters in the stable but more in the plastic. We detail the operations in the following. We denote the learnable parameters as  $\eta$  and  $\phi$  for the plastic and stable blocks respectively (at any CIL phase).  $\eta$  contains all the convolutional weights, while  $\phi$  contains only the neuron-level scaling weights (Sun et al., 2019) which are applied on the frozen convolutional neural network  $\theta_{\text{base}}$  pre-learned at the 0-th phase<sup>2</sup>. As a result, the number of learnable parameters  $\phi$  is much less than that of  $\eta$ . For example, when using the neurons of size  $3 \times 3$  in  $\theta_{\text{base}}$ , the number of learnable parameters  $\phi$  is reduced to only  $\frac{1}{3 \times 3}$  of the original number (i.e. the number of learnable parameters in  $\eta$ ).

**Feature extraction and aggregation.** Let  $\mathcal{F}_{\mu}^{[k]}(\cdot)$  denote the transformation function corresponding to the residual block with parameters  $\mu$  at Level  $k$ . Given a batch of training images  $x^{[0]}$ , we feed them to MANets and compute the feature maps at the  $k$ -th level (through the stable and plastic blocks respectively) as follows,

$$x_{\phi}^{[k]} = \mathcal{F}_{\phi \odot \theta_{\text{base}}}^{[k]}(x^{[k-1]}); \quad x_{\eta}^{[k]} = \mathcal{F}_{\eta}^{[k]}(x^{[k-1]}). \quad (1)$$

The transferabilities (of the knowledge learned from old classes) are different at different levels of neural networks (Yosinski et al., 2014). Therefore, it is important to apply different aggregating weights for different levels. Let  $\alpha_{\phi}^{[k]}$  and  $\alpha_{\eta}^{[k]}$  denote the aggregating weights of the stable and plastic blocks respectively at the  $k$ -th level, based on which we compute the weighted sum of  $x_{\phi}^{[k]}$  and  $x_{\eta}^{[k]}$  as follows,

$$x^{[k]} = \alpha_{\phi}^{[k]} \cdot x_{\phi}^{[k]} + \alpha_{\eta}^{[k]} \cdot x_{\eta}^{[k]}. \quad (2)$$

In our illustrative example in Figure 2(a), there are three pairs of weights at each phase. Hence, it becomes increasingly challenging to determine all the weights/hyperparameters if multiple phases are

<sup>2</sup>Related works (Hou et al., 2019; Douillard et al., 2020; Liu et al., 2020) learned  $\Theta_0$  in the 0-th phase using half of the total classes. We follow the same way to train  $\Theta_0$  and then freeze it as  $\theta_{\text{base}}$ .

involved. In this paper, we propose a meta-learning strategy to automatically adapt these weights, i.e., meta-optimizing the weights for different blocks at each phase, see details in Section 3.2.

**Highway connection blocks.** Highway network aims to address the vanishing gradients problem in deep neural networks (Srivastava et al., 2015). From the view of the network architecture, adding highway connection modifies our dual-block architecture to be a residual one where the highway plays the role of an identity branch (except that it has a gating mechanism) (He et al., 2016a). In specific, at each residual level, we add a block of  $1 \times 1$  convolution layers (stride=2) and denote it as  $h$ . We thus can rewrite Eq. 2 as follows,

$$x^{[k]} = \alpha_\phi^{[k]} \cdot x_\phi^{[k]} + \alpha_\eta^{[k]} \cdot x_\eta^{[k]} + x_h^{[k]}, \quad \text{where } x_h^{[k]} = \mathcal{F}_h^{[k]}(x^{[k-1]}). \quad (3)$$

When there are  $K$  levels in MANets (with or without highway at each level), we use the feature maps after the highest level  $x^{[K]}$  to train classifiers.

### 3.2 BILEVEL OPTIMIZATION PROGRAM FOR MANets

In each incremental phase, we optimize two groups of learnable parameters in MANets: (a) the scaling weights  $\phi$  on stable blocks, the convolutional weights  $\eta$  on plastic blocks, and the convolutional weights  $h$  on highway blocks; (b) the aggregating weights  $\alpha$ . The former is for network parameters and the latter is for hyperparameters. Therefore, we formulate the overall optimization process as a bilevel optimization program (BOP) (Goodfellow et al., 2014; Liu et al., 2020).

**BOP formulation.** In our MANets, the network parameters  $[\phi, \eta, h]$  are trained using the aggregating weights  $\alpha$  as hyperparameters. In turn,  $\alpha$  can be updated based on the learned network parameters  $[\phi, \eta, h]$ . In this way, the optimality of  $[\phi, \eta, h]$  imposes a constraint on  $\alpha$  and vice versa. Ideally, in the  $i$ -th phase, the CIL system aims to learn the optimal  $\alpha_i$  and  $[\phi_i, \eta_i, h_i]$  that minimize the classification loss on all training samples seen so far, i.e.,  $\mathcal{D}_i \cup \mathcal{D}_{0:i-1}$ , so the (ideal) BOP can be formulated as,

$$\min_{\alpha_i} \mathcal{L}(\alpha_i, \phi_i^*, \eta_i^*, h_i^*; \mathcal{D}_{0:i-1} \cup \mathcal{D}_i) \quad (4a)$$

$$\text{s.t. } [\phi_i^*, \eta_i^*, h_i^*] = \arg \min_{[\phi_i, \eta_i, h_i]} \mathcal{L}(\alpha_i, \phi_i, \eta_i, h_i; \mathcal{D}_{0:i-1} \cup \mathcal{D}_i), \quad (4b)$$

where  $\mathcal{L}(\cdot)$  denotes the loss function, e.g., cross-entropy loss. Please note that for the conciseness of the formulation, we use  $\phi_i$  to represent  $\phi_i \odot \theta_{\text{base}}$  (same in the follows). Following Liu et al. (2020), we call Problem 4a and Problem 4b as *meta-level* and *base-level* problems, respectively.

**Data strategy.** To solve Problem 4, we need to use  $\mathcal{D}_{0:i-1}$ . However, in the setting of CIL (Rebuffi et al., 2017; Hou et al., 2019; Douillard et al., 2020), we cannot access  $\mathcal{D}_{0:i-1}$  but only a small set of exemplars  $\mathcal{E}_{0:i-1}$ , e.g., 20 samples of each old class. Directly replacing  $\mathcal{D}_{0:i-1} \cup \mathcal{D}_i$  with  $\mathcal{E}_{0:i-1} \cup \mathcal{D}_i$  in Problem 4 will lead to the forgetting problem for the old classes. To alleviate this, we propose a new data strategy in which we use different training data splits to learn different parameters: (i) in the *meta-level* problem,  $\alpha_i$  is used to balance the stable and the plastic blocks, so we use the balanced subset to update it, i.e., meta-training  $\alpha_i$  on  $\mathcal{E}_{0:i-1} \cup \mathcal{E}_i$ ; (ii) in the *base-level* problem,  $[\phi_i, \eta_i, h_i]$  are the network parameters used for feature extraction, so we leverage all the available data to learn them, i.e., base-training  $[\phi_i, \eta_i, h_i]$  on  $\mathcal{E}_{0:i-1} \cup \mathcal{D}_i$ . In this way, we reformulate the ideal BOP in Problem 4 as a solvable BOP provided below,

$$\min_{\alpha_i} \mathcal{L}(\alpha_i, \phi_i^*, \eta_i^*, h_i^*; \mathcal{E}_{0:i-1} \cup \mathcal{E}_i) \quad (5a)$$

$$\text{s.t. } [\phi_i^*, \eta_i^*, h_i^*] = \arg \min_{[\phi_i, \eta_i, h_i]} \mathcal{L}(\alpha_i, \phi_i, \eta_i, h_i; \mathcal{E}_{0:i-1} \cup \mathcal{D}_i). \quad (5b)$$

**Updating parameters.** We solve the BOP by updating the two groups of parameters ( $\alpha_i$  and  $[\phi, \eta, h]$ ) alternatively across epochs, i.e., the  $j$ -th epoch for learning one group and the  $(j+1)$ -th epoch for the other group until both groups converge. First, we initialize  $\alpha_i, \phi_i, \eta_i$  and  $h_i$  with  $\alpha_{i-1}, \phi_{i-1}, \eta_{i-1}$  and  $h_{i-1}$ , respectively. Please note that  $\phi_0$  is initialized with ones, following Sun et al. (2019),  $\eta_0$  is initialized with  $\theta_{\text{base}}$ , and  $\alpha_0$  is initialized with 0.5. Based on our **Data strategy**, we use all available data in the  $i$ -th phase to solve the *base-level* problem, i.e., base-learning  $[\phi_i, \eta_i, h_i]$  as follows,

$$[\phi_i, \eta_i, h_i] \leftarrow [\phi_i, \eta_i, h_i] - \gamma_1 \nabla_{[\phi_i, \eta_i, h_i]} \mathcal{L}(\alpha_i, \phi_i, \eta_i, h_i; \mathcal{E}_{0:i-1} \cup \mathcal{D}_i). \quad (6)$$

Then, we use a balanced exemplar set to solve *meta-level* problem, i.e., meta-learning  $\alpha_i$  as follows,

$$\alpha_i \leftarrow \alpha_i - \gamma_2 \nabla_{\alpha_i} \mathcal{L}(\alpha_i, \phi_i, \eta_i, h_i; \mathcal{E}_{0:i-1} \cup \mathcal{E}_i), \quad (7)$$

where  $\gamma_1$  and  $\gamma_2$  are the *base-level* and *meta-level* learning rates, respectively. Algorithm 1 summarizes the training algorithm of the proposed MANets, taking the  $i$ -th CIL phase as an example.

## 4 EXPERIMENTS

We evaluate the proposed MANets on three CIL benchmarks, i.e., CIFAR-100 (Krizhevsky et al., 2009), ImageNet-Subset (Rebuffi et al., 2017) and ImageNet (Russakovsky et al., 2015), and achieve the state-of-the-art performance. Below we describe the datasets and implementation details (Section 4.1), followed by the results and analyses (Section 4.2) including comparisons to related methods, ablation studies and visualization results.

### 4.1 DATASETS AND IMPLEMENTATION DETAILS

**Datasets.** We conduct CIL experiments on two datasets, CIFAR-100 (Krizhevsky et al., 2009) and ImageNet (Russakovsky et al., 2015), following related works (Hou et al., 2019; Liu et al., 2020; Douillard et al., 2020). ImageNet is used in two CIL settings: one based on a subset of 100 classes (ImageNet-Subset) and the other based on the entire 1,000 classes. The 100-class data for ImageNet-Subset are randomly sampled from ImageNet with an identical random seed (1993) by NumPy, following Hou et al. (2019); Liu et al. (2020).

**Implementation details.** Following the uniform setting (Douillard et al., 2020; Liu et al., 2020), we use a 32-layer ResNet for CIFAR-100 and an 18-layer ResNet for ImageNet. The learning rates  $\gamma_1$  and  $\gamma_2$  are initialized as 0.1 and  $1 \times 10^{-5}$ , respectively. We impose a constraint on  $\alpha$ , i.e.,  $\alpha_\eta + \alpha_\phi = 1$  for each block. For CIFAR-100 (ImageNet), we train the model for 160 (90) epochs in each phase, and the learning rates are divided by 10 after 80 (30) and 120 (60) epochs. We use an SGD optimizer with momentum to train the model.

**Benchmark protocol.** This work follows the protocol in Hou et al. (2019), Liu et al. (2020), and Douillard et al. (2020). Given a dataset, the model is firstly trained on half of the classes. Then, it learns the remaining classes evenly in the subsequent phases. Assume there is an initial phase and  $N$  incremental phases for the CIL system.  $N$  is set to be 5, 10 or 25. At each phase, the model is evaluated on the test data for all seen classes. The average accuracy (over all phases) is reported.

### 4.2 RESULTS AND ANALYSES

Table 1 shows the results of 4 baselines with and without our MANets as a plug-in architecture, and some other related works. Table 2 demonstrates the results in 8 ablative settings. Figure 3 visualizes the Grad-CAM (Selvaraju et al., 2017) activation maps obtained from different residual blocks. Figure 4 shows our phase-wise results compared to those of baselines. Figure 5 shows the changes of values for  $\alpha_\eta$  and  $\alpha_\phi$  across 10 incremental phases.

**Comparing with the state-of-the-arts.** Table 1 shows that taking our MANets as a plug-in architecture on 4 baseline methods (Rebuffi et al., 2017; Hou et al., 2019; Liu et al., 2020; Douillard et al., 2020) consistently improves their performance. E.g., on CIFAR-100, “LUCIR + MANets” achieves 3% of improvement on average. In Figure 4, we can observe that our method achieves the highest accuracy in all settings, compared to the state-of-the-arts. Interestingly, we find that our MANets can boost the more performance for the simpler baseline methods, e.g., iCaRL. “iCaRL + MANets” achieves better results than those of LUCIR on ImageNet-Subset, even though the latter method uses a series of regularization techniques.

---

#### Algorithm 1 MANets (in the $i$ -th phase)

---

- 1: **Input:** New class data  $\mathcal{D}_i$ ; old class exemplars  $\mathcal{E}_{0:i-1}$ ; old parameters  $\alpha_{i-1}$ ,  $\phi_{i-1}$ ,  $\eta_{i-1}$ , and  $h_{i-1}$ ; base model  $\theta_{\text{base}}$ .
  - 2: **Output:** new parameters  $\alpha_i$ ,  $\phi_i$ ,  $\eta_i$ , and  $h_i$ ; new class exemplars  $\mathcal{E}_i$ .
  - 3: Get  $\mathcal{D}_i$  and load  $\mathcal{E}_{0:i-1}$  from memory;
  - 4: Initialize  $[\phi_i, \eta_i, h_i]$  with  $[\phi_{i-1}, \eta_{i-1}, h_{i-1}]$ ;
  - 5: Initialize  $\alpha_i$  with  $\alpha_{i-1}$ ;
  - 6: Select exemplars  $\mathcal{E}_i \subseteq \mathcal{D}_i$  by herding;
  - 7: **for** epochs **do**
  - 8:   **for** *mini-batch* **in**  $\mathcal{E}_{0:i-1} \cup \mathcal{D}_i$  **do**
  - 9:     Train  $[\phi_i, \eta_i, h_i]$  on  $\mathcal{E}_{0:i-1} \cup \mathcal{D}_i$  by Eq. 6;
  - 10:   **end for**
  - 11:   **for** *mini-batch* **in**  $\mathcal{E}_{0:i-1} \cup \mathcal{E}_i$  **do**
  - 12:     Meta-train  $\alpha_i$  on  $\mathcal{E}_{0:i-1} \cup \mathcal{E}_i$  by Eq. 7;
  - 13:   **end for**
  - 14: **end for**
  - 15: Update exemplars  $\mathcal{E}_i$  by herding;
  - 16: Replace  $\mathcal{E}_{0:i-1}$  with  $\mathcal{E}_{0:i-1} \cup \mathcal{E}_i$  in the memory.
-

Method	CIFAR-100			ImageNet-Subset			ImageNet		
	$N=5$	10	25	5	10	25	5	10	25
LwF (Li & Hoiem, 2018)	49.59	46.98	45.51	53.62	47.64	44.32	44.35	38.90	36.87
BiC (Wu et al., 2019)	59.36	54.20	50.00	70.07	64.96	57.73	62.65	58.72	53.47
TPCIL (Tao et al., 2020)	65.34	63.58	–	76.27	74.81	–	64.89	62.88	–
iCaRL (Rebuffi et al., 2017)	57.12	52.66	48.22	65.44	59.88	52.97	51.50	46.89	43.14
+ MANets (ours)	64.11	60.22	56.40	73.42	71.76	69.21	63.74	61.19	56.92
LUCIR (Hou et al., 2019)	63.17	60.14	57.54	70.84	68.32	61.44	64.45	61.57	56.56
+ MANets (ours)	67.12	65.21	<b>64.29</b>	73.25	72.19	70.95	64.62	62.22	60.60
Mnemonics (Liu et al., 2020)	63.34	62.28	60.96	72.58	71.37	69.74	64.54	63.01	61.00
+ MANets (ours)	<b>67.37</b>	<b>65.64</b>	63.29	73.13	72.06	70.75	64.90	63.42	<b>61.45</b>
PODNet-CNN (Douillard et al., 2020)	64.83	63.19	60.72	75.54	74.33	68.31	66.95	64.13	59.17
+ MANets (ours)	66.12	64.11	62.12	<b>76.63</b>	<b>75.40</b>	<b>71.43</b>	<b>67.60</b>	<b>64.79</b>	60.97

Table 1: Average incremental accuracy (%) of four CIL methods with and without our MANets as a plug-in architecture, and the related methods. Please note (1) Douillard et al. (2020) didn’t report the results for  $N=25$  on the ImageNet, so we produce the results using their public code; (2) Liu et al. (2020) updated the results on arXiv version (after fixing a bug in their code), different from its conference version; (3) Highway connection blocks are applied in our MANets; and (4) For CIFAR-100, we use “all”+“scaling” blocks. For ImageNet-Subset and ImageNet, we use “scaling”+“frozen” blocks. Please refer to Section 4.2 **Ablation settings** for details.

**Ablation settings.** Table 2 demonstrates the ablation study. **Block types:** by differentiating the numbers of learnable parameters, we have 3 block types: (1) “all” means learning all the convolutional weights and biases; (2) “scaling” means learning neuron-level scaling weights (Sun et al., 2019) on the top of a frozen base model  $\theta_{\text{base}}$ ; and (3) “frozen” means using  $\theta_{\text{base}}$  (frozen) as the feature extractor of the stable block. Rows 1 is the baseline model of LUCIR (Hou et al., 2019). Row 2 is a double-block version of LUCIR. They are without meta-learning. Rows 3-5 are our MANets using different pairs of blocks. Row 6-8 use “all”+“scaling”, and under the setting of: (1) Row 6 includes highway connection blocks; (2) Row 7 uses imbalanced data  $\mathcal{E}_{0:i-1} \cup \mathcal{D}_i$  to meta-train  $\alpha$ ; and (3) Row 8 simply uses fixed weights  $\alpha_\eta = 0.5$  and  $\alpha_\phi = 0.5$  at each residual level.

Row	Ablation Setting	CIFAR-100			ImageNet-Subset		
		$N=5$	10	25	5	10	25
1	only single “all”	63.17	60.14	57.54	70.84	68.32	61.44
2	“all” + “all”	64.49	61.89	58.87	69.72	66.69	63.29
3	“all” + “scaling”	66.21	65.17	63.45	71.38	69.11	67.40
4	“all” + “frozen”	65.62	64.05	63.67	71.71	69.87	67.92
5	“scaling” + “frozen”	64.71	63.65	62.89	<b>73.01</b>	<b>71.65</b>	<b>70.30</b>
6	w/ highway	<b>67.12</b>	<b>65.21</b>	<b>64.29</b>	71.98	70.36	69.35
7	w/o balanced $\mathcal{E}$	65.91	64.70	63.08	70.30	69.92	66.89
8	w/o meta-learned $\alpha$	65.89	64.49	62.89	70.31	68.71	66.34

Table 2: Ablation results (%). The baseline (Row 1) is LUCIR. Meta-learned  $\alpha$  are applied for Rows 3-7. Rows 6-8 are based on “all”+“scaling”. Note that highway connection blocks are applied only on Row 6.

**Ablation results.** Comparing the second block of results (Rows 3-5) to the first block (baseline), it is obvious that using the proposed MANets can significantly improve the performance of incremental learning, e.g. an average of over 6% gain on ImageNet-Subset ( $N = 25$ ). From Rows 3-5, we can observe that on ImageNet-Subset, the model with fewer learnable parameters (“scaling”+“frozen”) works the best. This is because we use a shallower network for the larger dataset following the benchmark protocol (ResNet-32 for CIFAR-100; ResNet-18 for ImageNet-Subset), so  $\theta_{\text{base}}$  for ImageNet-Subset is well-learned in the initial phase and can offer high-quality features for later phases. Comparing Row 6 to Row 3, it is clear that highway connection is helpful for all settings. Comparing Row 7 to Row 3, it shows the importance of using balanced subset to meta-optimize  $\alpha$ . Comparing Row 8 to Row 3, it shows the superiority of meta-learned  $\alpha$  (that is dynamic and optimal) over manually-chosen  $\alpha$ .



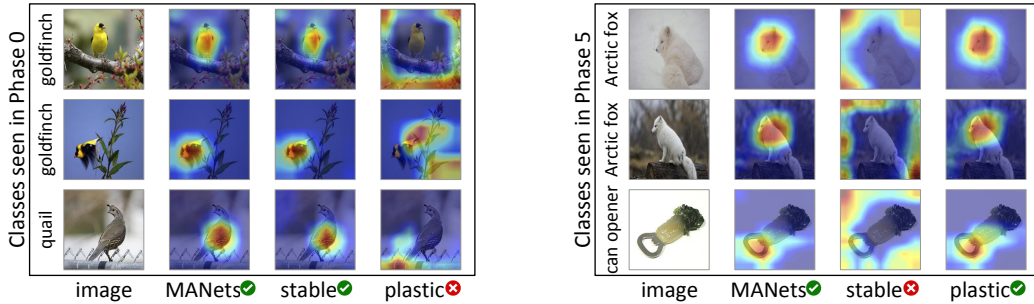


Figure 3: The activation maps using Grad-CAM (Selvaraju et al., 2017) for Phase 5 (the last phase) model on ImageNet-Subset ( $N=5$ ). Samples are selected from the classes coming in Phase 0 (left) and Phase 5 (right), respectively. Green tick (red cross) means the discriminative features are activated on the object regions successfully (unsuccessfully).  $\bar{\alpha}_\eta = 0.428$  and  $\bar{\alpha}_\phi = 0.572$ .

### The visualization of activation maps.

Figure 3 shows the activation maps visualized by Grad-CAM for Phase 5 (last phase) model on ImageNet-Subset ( $N=5$ ). The visualized samples (on the left and right) are from the classes coming in Phase 0 and Phase 5, respectively. When input Phase 0 samples to the Phase 5 model, it activates the object regions on the stable block but fails on the plastic block. It is easy to explain as the plastic block already forgets the knowledge learned in Phase 0 while the stable block successfully retains it. This situation is reversed when input Phase 5 samples to that model. It is because the stable block is far less learnable and fails to adapt to the new coming data. While for all samples, our MANets can capture the right object features, as it aggregates the feature maps from two types of blocks and its meta-learned aggregating weights ensure the effective adaptation (balancing between two types of blocks) in both early and late phases.

**The values of  $\alpha_\eta$  and  $\alpha_\phi$ .** Figure 5 shows the changes of values for  $\alpha_\eta$  and  $\alpha_\phi$  on CIFAR-100 ( $N=10$ ). We can see that Level 1 tends to get larger values of  $\alpha_\phi$ , while Level 3 tends to get larger values of  $\alpha_\eta$ , i.e., lower-level residual block learns to be stabler which is intuitively correct in deep models. Actually, the CIL system is continuously transferring its learned knowledge to subsequent phases. Different layers (or levels) of the model have different transferabilities (Yosinski et al., 2014). Level 1 encodes low-level features that are more stable and shareable among classes. Level 3 nears the classifiers, and it tends to be more plastic such as to fast to adapt to new coming data.

## 5 CONCLUSIONS

In this paper, we introduce a novel network architecture MANets for class-incremental learning (CIL). Our main contribution lies in addressing the issue of stability-plasticity dilemma by aggregating the feature maps from two types of residual blocks (i.e., stable and plastic blocks). To enable the automated and adaptive aggregation, we meta-learn the weights for different types of blocks (and at different levels) in an end-to-end manner. Our approach is *generic* and can be easily incorporated into existing CIL methods to boost the performance.

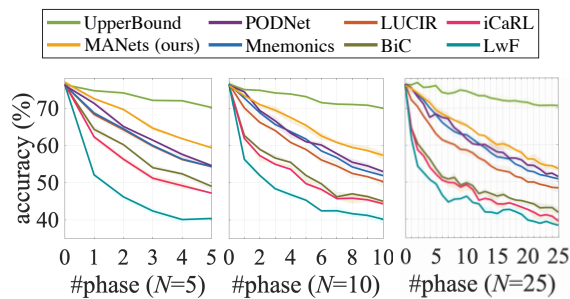


Figure 4: Phase-wise accuracy on CIFAR-100. “Upper Bound” shows the results of joint training with all previous data accessible in each phase. The average accuracy of each curve is reported in Table 1, and our results are on the row of “Mnemonics + MANets”.

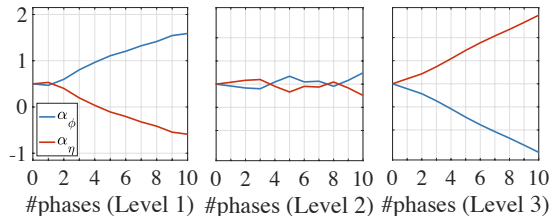


Figure 5: The changes of values for  $\alpha_\eta$  and  $\alpha_\phi$  on CIFAR-100 ( $N=10$ ). All curves are smoothed with a rate of 0.8 for a better visualization. More results are provided in the appendices (Figures S2 and S3).



---

## REFERENCES

- Davide Abati, Jakub Tomczak, Tijmen Blankevoort, Simone Calderara, Rita Cucchiara, and Babak Ehteshami Bejnordi. Conditional channel gated networks for task-aware continual learning. In *CVPR*, pp. 3931–3940, 2020.
- Rahaf Aljundi, Punarjay Chakravarty, and Tinne Tuytelaars. Expert gate: Lifelong learning with a network of experts. In *CVPR*, pp. 3366–3375, 2017.
- Francisco M. Castro, Manuel J. Marín-Jiménez, Nicolás Guil, Cordelia Schmid, and Karteek Alahari. End-to-end incremental learning. In *ECCV*, pp. 241–257, 2018.
- Arslan Chaudhry, Marc’Aurelio Ranzato, Marcus Rohrbach, and Mohamed Elhoseiny. Efficient lifelong learning with a-gem. In *ICLR*, 2019.
- Zhiyuan Chen and Bing Liu. Lifelong machine learning. *Synthesis Lectures on Artificial Intelligence and Machine Learning*, 12(3):1–207, 2018.
- Matthias De Lange, Rahaf Aljundi, Marc Masana, Sarah Parisot, Xu Jia, Aleš Leonardis, Gregory Slabaugh, and Tinne Tuytelaars. A continual learning survey: Defying forgetting in classification tasks. *arXiv*, 1909.08383, 2019a.
- Matthias De Lange, Rahaf Aljundi, Marc Masana, Sarah Parisot, Xu Jia, Ales Leonardis, Gregory Slabaugh, and Tinne Tuytelaars. Continual learning: A comparative study on how to defy forgetting in classification tasks. *arXiv*, 1909.08383, 2019b.
- Arthur Douillard, Matthieu Cord, Charles Ollion, Thomas Robert, and Eduardo Valle. Podnet: Pooled outputs distillation for small-tasks incremental learning. In *ECCV*, 2020.
- Chelsea Finn, Pieter Abbeel, and Sergey Levine. Model-agnostic meta-learning for fast adaptation of deep networks. In *ICML*, pp. 1126–1135, 2017.
- Ian Goodfellow, Jean Pouget-Abadie, Mehdi Mirza, Bing Xu, David Warde-Farley, Sherjil Ozair, Aaron Courville, and Yoshua Bengio. Generative adversarial nets. In *NIPS*, pp. 2672–2680, 2014.
- Kaiming He, Xiangyu Zhang, Shaoqing Ren, and Jian Sun. Identity mappings in deep residual networks. In Bastian Leibe, Jiri Matas, Nicu Sebe, and Max Welling (eds.), *ECCV*, pp. 630–645. Springer, 2016a.
- Kaiming He, Xiangyu Zhang, Shaoqing Ren, and Jian Sun. Deep residual learning for image recognition. In *CVPR*, pp. 770–778, 2016b.
- Geoffrey E. Hinton, Oriol Vinyals, and Jeffrey Dean. Distilling the knowledge in a neural network. *arXiv*, 1503.02531, 2015.
- Saihui Hou, Xinyu Pan, Chen Change Loy, Zilei Wang, and Dahua Lin. Learning a unified classifier incrementally via rebalancing. In *CVPR*, pp. 831–839, 2019.
- Wenpeng Hu, Zhou Lin, Bing Liu, Chongyang Tao, Zhengwei Tao, Jinwen Ma, Dongyan Zhao, and Rui Yan. Overcoming catastrophic forgetting for continual learning via model adaptation. In *ICLR*, 2019.
- Ronald Kemker, Marc McClure, Angelina Abitino, Tyler L. Hayes, and Christopher Kanan. Measuring catastrophic forgetting in neural networks. In *AAAI*, pp. 3390–3398, 2018.
- Alex Krizhevsky, Geoffrey Hinton, et al. Learning multiple layers of features from tiny images. Technical report, Citeseer, 2009.
- Zhizhong Li and Derek Hoiem. Learning without forgetting. *IEEE Transactions on Pattern Analysis and Machine Intelligence*, 40(12):2935–2947, 2018.
- Yaoyao Liu, Yuting Su, An-An Liu, Bernt Schiele, and Qianru Sun. Mnemonics training: Multi-class incremental learning without forgetting. In *CVPR*, pp. 12245–12254, 2020.

- 
- David Lopez-Paz and Marc’Aurelio Ranzato. Gradient episodic memory for continual learning. In *NIPS*, pp. 6467–6476, 2017.
- Matthew MacKay, Paul Vicol, Jon Lorraine, David Duvenaud, and Roger Grosse. Self-tuning networks: Bilevel optimization of hyperparameters using structured best-response functions. In *ICLR*, 2019.
- Michael McCloskey and Neal J Cohen. Catastrophic interference in connectionist networks: The sequential learning problem. In *Psychology of Learning and Motivation*, volume 24, pp. 109–165. Elsevier, 1989.
- K. McRae and P. Hetherington. Catastrophic interference is eliminated in pre-trained networks. In *CogSci*, 1993.
- Martial Mermillod, Aurélie Bugaiska, and Patrick Bonin. The stability-plasticity dilemma: Investigating the continuum from catastrophic forgetting to age-limited learning effects. *Frontiers in Psychology*, 4:504, 2013.
- Ameya Prabhu, Philip HS Torr, and Puneet K Dokania. Gdumb: A simple approach that questions our progress in continual learning. In *ECCV*, 2020.
- Jathushan Rajasegaran, Munawar Hayat, Salman H Khan, Fahad Shahbaz Khan, and Ling Shao. Random path selection for continual learning. In *NeurIPS*, pp. 12669–12679, 2019.
- Jathushan Rajasegaran, Salman Khan, Munawar Hayat, Fahad Shahbaz Khan, and Mubarak Shah. itaml: An incremental task-agnostic meta-learning approach. In *CVPR*, pp. 13588–13597, 2020.
- R. Ratcliff. Connectionist models of recognition memory: Constraints imposed by learning and forgetting functions. *Psychological Review*, 97:285–308, 1990.
- Sylvestre-Alvise Rebuffi, Alexander Kolesnikov, Georg Sperl, and Christoph H Lampert. iCaRL: Incremental classifier and representation learning. In *CVPR*, pp. 5533–5542, 2017.
- Matthew Riemer, Ignacio Cases, Robert Ajemian, Miao Liu, Irina Rish, Yuhai Tu, and Gerald Tesauro. Learning to learn without forgetting by maximizing transfer and minimizing interference. In *ICLR*, 2019.
- Olga Russakovsky, Jia Deng, Hao Su, Jonathan Krause, Sanjeev Satheesh, Sean Ma, Zhiheng Huang, Andrej Karpathy, Aditya Khosla, Michael Bernstein, et al. Imagenet large scale visual recognition challenge. *International Journal of Computer Vision*, 115(3):211–252, 2015.
- Ramprasaath R Selvaraju, Michael Cogswell, Abhishek Das, Ramakrishna Vedantam, Devi Parikh, and Dhruv Batra. Grad-cam: Visual explanations from deep networks via gradient-based localization. In *CVPR*, pp. 618–626, 2017.
- Hanul Shin, Jung Kwon Lee, Jaehong Kim, and Jiwon Kim. Continual learning with deep generative replay. In *NIPS*, pp. 2990–2999, 2017.
- Ankur Sinha, Pekka Malo, and Kalyanmoy Deb. A review on bilevel optimization: From classical to evolutionary approaches and applications. *IEEE Transactions on Evolutionary Computation*, 22(2):276–295, 2018.
- Rupesh Kumar Srivastava, Klaus Greff, and Jürgen Schmidhuber. Training very deep networks. In Corinna Cortes, Neil D. Lawrence, Daniel D. Lee, Masashi Sugiyama, and Roman Garnett (eds.), *NIPS*, pp. 2377–2385, 2015.
- Qianru Sun, Yaoyao Liu, Tat-Seng Chua, and Bernt Schiele. Meta-transfer learning for few-shot learning. In *CVPR*, pp. 403–412, 2019.
- Xiaoyu Tao, Xinyuan Chang, Xiaopeng Hong, Xing Wei, and Yihong Gong. Topology-preserving class-incremental learning. In *ECCV*, 2020.
- Heinrich Von Stackelberg and Stackelberg Heinrich Von. *The theory of the market economy*. Oxford University Press, 1952.

---

Tongzhou Wang, Jun-Yan Zhu, Antonio Torralba, and Alexei A. Efros. Dataset distillation. *arXiv*, 1811.10959, 2018.

Max Welling. Herding dynamical weights to learn. In *ICML*, pp. 1121–1128, 2009.

Yue Wu, Yinpeng Chen, Lijuan Wang, Yuancheng Ye, Zicheng Liu, Yandong Guo, and Yun Fu. Large scale incremental learning. In *CVPR*, pp. 374–382, 2019.

Jason Yosinski, Jeff Clune, Yoshua Bengio, and Hod Lipson. How transferable are features in deep neural networks? In *NIPS*, pp. 3320–3328, 2014.

---

## APPENDICES

The appendices include more ablation results (§A), additional phase-wise accuracy plots (§B), additional plots for  $\alpha_\eta$  and  $\alpha_\phi$  values (§C), and the scaling weights (§D).

### A MORE ABLATION RESULTS

In Table S1, we supplement the ablation results for more settings. By differentiating the numbers of learnable parameters, we have three different types of blocks: By differentiating the numbers of learnable parameters, we have 3 block types: (1) “all” means learning all the convolutional weights and biases; (2) “scaling” means learning neuron-level scaling weights (Sun et al., 2019) on the top of a frozen base model  $\theta_{\text{base}}$ ; and (3) “frozen” means using  $\theta_{\text{base}}$  (frozen) as the feature extractor of the stable block. Please note that the classification layers are always learnable. “2×” (“4×”) means using an expanded network with two (four) branches with the same type residual blocks. We can observe that using two types of blocks (Rows 7-9) achieves better performance compared to using a double-sized or quadruple-sized model using the same blocks.

Row	Ablation Setting	CIFAR-100		
		N=5	10	25
1	1× “all”	63.17	60.14	57.54
2	2× “all”	64.49	61.89	58.87
3	4× “all”	65.70	62.31	59.40
4	1× “scaling”	62.48	61.53	60.17
5	2× “scaling”	65.13	64.08	62.50
6	4× “scaling”	66.00	64.67	63.67
7	“all” + “frozen”	65.62	64.05	<b>63.67</b>
8	“scaling” + “frozen”	64.71	63.65	62.89
9	“all” + “scaling”	<b>66.21</b>	<b>65.17</b>	63.45

Table S1: More ablation results (%).

### B ADDITIONAL PHASE-WISE ACCURACY PLOTS

In Figures S1, we supplement phase-wise accuracy on ImageNet-Subset and ImageNet, respectively. “Upper Bound” shows the results of joint training with all previous data accessible in each phase. We can observe that our method achieves the highest average accuracy in all settings.

### C ADDITIONAL PLOTS FOR $\alpha_\eta$ AND $\alpha_\phi$ VALUES

In Figures S2 and S3, we supplement the plots  $\alpha_\eta$  and  $\alpha_\phi$  values on CIFAR-100 and ImageNet-Subset. All curves are smoothed with a rate of 0.8 for a better visualization.

### D THE SCALING WEIGHTS

For stable blocks, we deploy the scaling weights  $\phi$ , which specifically transfer the base model  $\theta_{\text{base}}$ . The aim is to preserve the structural knowledge of  $\theta_{\text{base}}$  and slowly adapt  $\phi$  to the new class data. Specifically, we assume the  $q$ -th layer of  $\theta_{\text{base}}$  contains  $R$  neurons, so we have  $R$  neuron weights as  $\{W_{q,r}\}_{r=1}^R$ . For conciseness, we denote them as  $W_q$ . For  $W_q$ , we learn  $R$  scaling weights denoted as  $\phi_q$ . Let  $X_{q-1}$  and  $X_q$  be the input and output (feature maps) of the  $q$ -th layer. We apply  $\phi_q$  to  $W_q$  as,

$$X_q = (W_q \odot \phi_q)X_{q-1}, \quad (8)$$

where  $\odot$  donates the element-wise multiplication. Assuming there are  $Q$  layers in total, the scaling weights are denoted as  $\phi = \{\phi_q\}_{q=1}^Q$ .

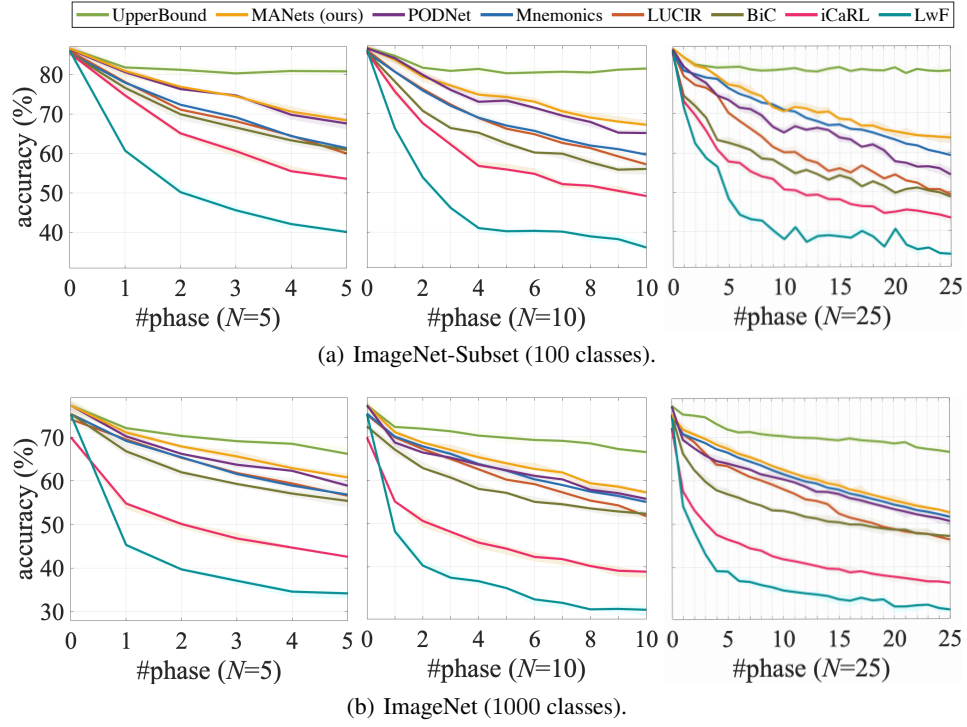


Figure S1: Phase-wise accuracy (%). The average accuracy of each curve is reported in Table 1, and our results are on the row of “PODNet-CNN + MANets”.

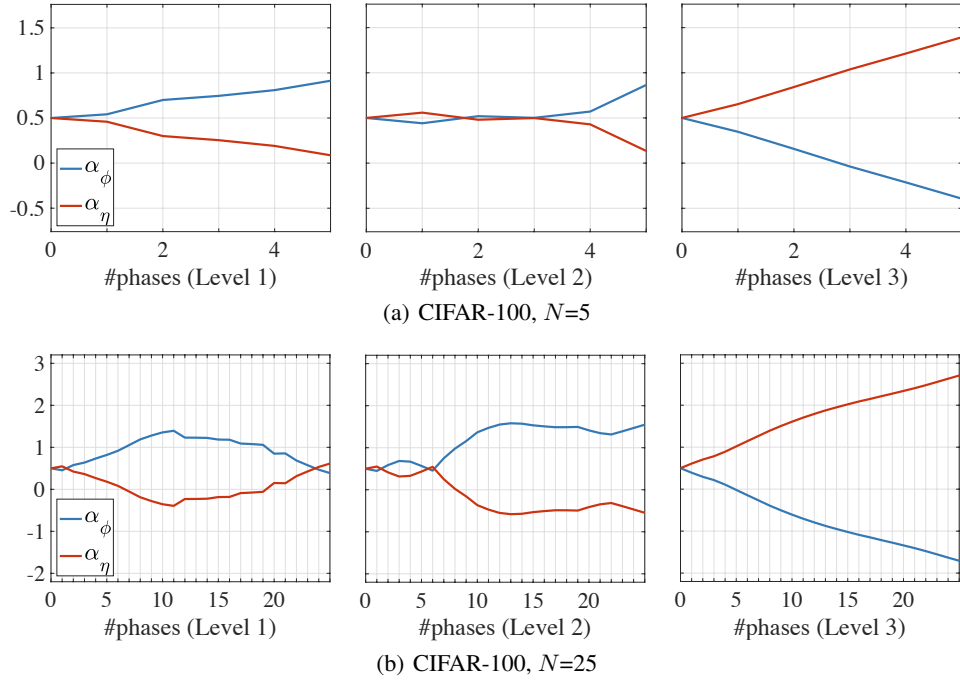


Figure S2: The changes of values for  $\alpha_\eta$  and  $\alpha_\phi$  on CIFAR-100.

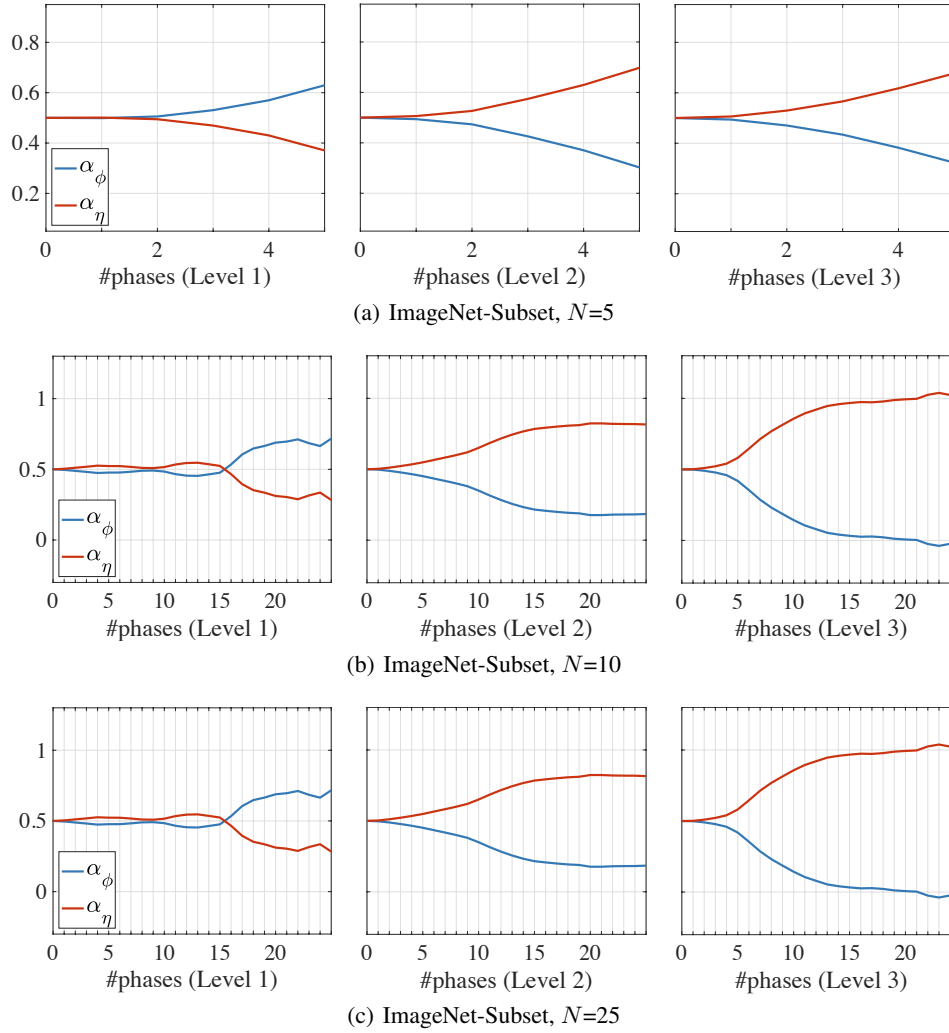


Figure S3: The changes of values for  $\alpha_\eta$  and  $\alpha_\phi$  on ImageNet-Subset.